

## Scaling of the Low-Energy Structure in Above-Threshold Ionization in the Tunneling Regime: Theory and Experiment

L. Guo,<sup>1</sup> S. S. Han,<sup>1</sup> X. Liu,<sup>2</sup> Y. Cheng,<sup>3</sup> Z. Z. Xu,<sup>3</sup> J. Fan,<sup>4,\*</sup> J. Chen,<sup>5,6,†</sup> and S. G. Chen<sup>6</sup>

<sup>1</sup>Key Laboratory for Quantum Optics and Center for Cold Atom Physics, Shanghai Institute of Optics and Fine Mechanics, Chinese Academy of Sciences, Shanghai 201800, China

<sup>2</sup>State Key Laboratory of Magnetic Resonance and Atomic and Molecular Physics, Wuhan Institute of Physics and Mathematics, Chinese Academy of Sciences, Wuhan 430071, China

<sup>3</sup>State Key Laboratory of High Field Laser Physics, Shanghai Institute of Optics and Fine Mechanics, Chinese Academy of Sciences, Shanghai 201800, China

<sup>4</sup>Joint Quantum Institute, University of Maryland, College Park, Maryland 20742, USA

<sup>5</sup>HEDPS, Center for Applied Physics and Technology, Peking University, Beijing 100084, China

<sup>6</sup>Institute of Applied Physics and Computational Mathematics, P. O. Box 8009, Beijing 100088, China

W. Becker

Max-Born-Institut, Max-Born-Strasse 2a, 12489 Berlin, Germany

C. I. Blaga, A. D. DiChiara, E. Sistrunk, P. Agostini, and L. F. DiMauro

Department of Physics, The Ohio State University, Columbus, Ohio 43210, USA

(Received 7 May 2012; published 2 January 2013)

A calculation of the second-order (rescattering) term in the  $S$ -matrix expansion of above-threshold ionization is presented for the case when the binding potential is the unscreened Coulomb potential. Technical problems related to the divergence of the Coulomb scattering amplitude are avoided in the theory by considering the depletion of the atomic ground state due to the applied laser field, which is well defined and does not require the introduction of a screening constant. We focus on the low-energy structure, which was observed in recent experiments with a midinfrared wavelength laser field. Both the spectra and, in particular, the observed scaling versus the Keldysh parameter and the ponderomotive energy are reproduced. The theory provides evidence that the origin of the structure lies in the long-range Coulomb interaction.

DOI: [10.1103/PhysRevLett.110.013001](https://doi.org/10.1103/PhysRevLett.110.013001)

PACS numbers: 33.80.Rv, 33.80.Wz, 42.50.Hz

Above-threshold ionization (ATI) is an important process in the interaction between atoms and an intense laser field [1,2]. The photoelectron energy spectrum shows that ATI occurs either in the form of multiphoton ionization or tunneling ionization. These two regimes can simply be distinguished by the value of the Keldysh parameter  $\gamma = \sqrt{I_p/2U_p}$  [3], where  $I_p$  is the ionization potential of the atom and  $U_p$  the ponderomotive energy of the laser field. In the multiphoton regime where  $\gamma > 1$ , the photoelectron spectrum consists of individual ATI peaks spaced by the energy of one photon with monotonically decreasing amplitude [1,4,5]. In the tunneling or over-the-barrier ionization regimes where  $\gamma \ll 1$ , the ATI photoelectron distribution is consistent with the classical simple-man picture [6,7]. The distribution in this case has an exponentially decreasing amplitude and a cutoff energy at  $2U_p$ . Beyond  $2U_p$  a flat plateau emerges and extends to a cutoff at  $10U_p$  [8] due to back-scattering of the ionized electron off the core [9,10]. The  $2U_p$  cutoff is well described by the first-order  $S$ -matrix theory [5], often referred to as the “strong-field approximation” (SFA) [3,5,11]. However, this

approximation cannot account for the high-energy plateau and the low-energy structure (LES), which is the focus of this Letter.

One finding deviating from the SFA prediction is the observed low-energy momentum distribution [12,13] of the recoiling ions. Several explanations have been proposed and are still under debate, tracing the effect to the long-range Coulomb potential [14–16], Freeman resonances [17,18], or the persistence of ATI peaks in the tunneling regime [19,20]. Recently, another unexpected LES has been reported in the ATI electron-energy distribution, which becomes most significant at longer wavelength or decreasing  $\gamma < 1$  [21,22]. This LES is in stark contrast to the prediction of the SFA model. A semiclassical model has qualitatively attributed the effect to the long-range Coulomb potential [22]. Calculations based on numerical solution of the 3D time-dependent Schrödinger equation (TDSE) [21] provide quantitative agreement but little physical insight. In this Letter, we present a heuristic analysis showing that the LES structure, which cannot be accounted for by the lowest-order  $S$ -matrix theory (i.e., the SFA), is reproduced by the second-order amplitude. The good agreement between our heuristic theory and the

experimental data supports the conclusion that the LES can be attributed to the dominance of the long-range electron–parent-ion Coulomb interaction in the tunneling regime.

In our calculation, the Hamiltonian related to photoionization is given by  $V_A + V$ , with  $V_A(t)$  the laser-atom interaction and  $V$  the electron-parent ion Coulomb interaction. The  $S$ -matrix expansion is [5]

$$(S - 1)_{fi} = T^{(1)} + T^{(2)} + \dots$$

$$= -i \int_{-\infty}^{\infty} dt \langle \Psi_{A_f}(\mathbf{p}, t) | V_A(t) | \varphi_i(t) \rangle \quad (1a)$$

$$+ (-i^2) \int_{-\infty}^{\infty} dt \int_{-\infty}^t dt' \int d^3 \mathbf{p}' \langle \Psi_{A_f}(\mathbf{p}, t) | V | \Psi_A(\mathbf{p}', t) \rangle \langle \Psi_A(\mathbf{p}', t') | V_A(t') | \varphi_i(t') \rangle + \dots, \quad (1b)$$

where  $|\varphi_i(t)\rangle = |\varphi_0\rangle e^{iI_p t}$  is the atomic ground state with  $I_p$  the ionization potential and  $|\Psi_{A_f}(\mathbf{p}, t)\rangle$  the Volkov wave function with the final electron momentum  $\mathbf{p}$ . The first term [Eq. (1a)] of this expansion is the standard SFA, which describes the “direct” electrons, which after they have been liberated do not interact with the binding potential anymore. The second term allows for just one such “rescattering” interaction, and each subsequent higher-order term contains one additional interaction  $V$ , with propagation in the presence of the laser field (Volkov propagation) in between.

The second term [Eq. (1b)] generates the ATI plateau. It exhibits a fivefold integration—two over time and one over the intermediate vector momentum—provided that the matrix elements of  $V$  and  $V_A$  can be evaluated analytically. Normally, these integrations are carried out by the method of steepest descent, which affords close contact with the classical “simple-man” model via the concept of quantum orbits. However, for very low momenta  $\mathbf{p}$ , which are the focus of this Letter, the reliability of this approximation is not clear. If we commute the integrals over the ionization time  $t'$  and the rescattering time  $t$  with the one over the intermediate momentum  $\mathbf{p}'$ , then the former two can be exactly evaluated and the rescattering amplitude [Eq. (1b)] is converted into the double sum

$$T^{(2)} \equiv \sum_N \delta(p^2/2 - \mathcal{E}_N) \int d^3 \mathbf{p}' \langle \mathbf{p} | V | \mathbf{p}' \rangle$$

$$\times \sum_n \frac{1}{p'^2/2 - \mathcal{E}_n - i\epsilon} f_{N,n}(\mathbf{p}, \mathbf{p}'), \quad (2)$$

where  $\mathcal{E}_n \equiv n\omega - I_p - U_p$  with  $U_p$  the ponderomotive potential and  $I_p$  the ionization potential. The  $\delta$  function comes from the integration over  $t$  and the energy denominator is the result of the integration over  $t'$ . The functions  $f_{N,n}(\mathbf{p}, \mathbf{p}')$  are sums over Bessel functions. In the current context, it is only important that they are nonsingular when  $p \rightarrow p'$ .

For a negative ion, where the electron is bound by a short-range potential, e.g., the Yukawa potential  $\exp(-\kappa r)/r$ , this procedure is straightforward. We have  $\langle \mathbf{p} | V | \mathbf{p}' \rangle \sim [(\mathbf{p} - \mathbf{p}')^2 + \kappa^2]^{-1}$ , and the spectra calculated from Eq. (2) for suitable  $\kappa$  agree very well with the experimental data

[23]. The second-order term  $T^{(2)}$  is much smaller than the first-order term  $T^{(1)}$ , and the higher-order terms are completely insignificant. For a Coulomb potential, however, we encounter a divergence, which originates from the singular behavior of the Coulomb scattering amplitude in the forward direction, which is now  $\langle \mathbf{p} | V | \mathbf{p}' \rangle \sim (\mathbf{p} - \mathbf{p}')^{-2}$ . Namely, for  $N = n$  the integral over  $\mathbf{p}'$  in Eq. (2) is now logarithmically divergent. This becomes clear if we substitute the energy denominator according to  $1/(x - i\epsilon) = P(1/x) + i\pi\delta(x)$ . The principal part does not contribute while the  $\delta$  function causes  $p = p'$  and, hence, the divergence mentioned. A second related problem is that, for the Coulomb potential, numerical estimates indicate that for low momenta  $T^{(2)}$  is larger than  $T^{(1)}$ , and the higher-order terms are likely to be larger still.

The latter situation is reminiscent of field-free Coulomb scattering, where the exact scattering amplitude is (see, e.g., Ref. [24])

$$f(\theta) = -\frac{\beta}{2p \sin^2(\theta/2)} \exp\{-i\beta \ln[\sin^2(\theta/2)]\} f_0, \quad (3)$$

with  $f_0 = \exp[2i \arg \Gamma(1 + i\beta)]$ ,  $\beta = Z/p$ ,  $\theta$  the scattering angle, and  $Z$  is the product of the projectile and the target charge. In an expansion in powers of  $Z$ , the lowest order gives the Rutherford amplitude. Higher-order terms exhibit logarithmically higher and higher orders of the forward-scattering singularity at  $\theta = 0$  so that each term is larger in magnitude than the previous one. However, as shown by Eq. (3), all of these terms sum to a phase, which drops out of the scattering cross section, which is proportional to  $|f(\theta)|^2$ , thus restoring the first-order Rutherford result. Terminating the expansion in terms of  $Z$  at any finite order beyond the first generates a result that is inferior to the one of first order.

This analysis cannot directly be repeated in the present much more complicated time-dependent case. However, it is very suggestive that the same mechanism is also hidden in the expansion (1). With this in mind, we focus on the second order  $T^{(2)}$  and ignore the higher-order terms. As mentioned above, evaluation of the second-order term is still impeded by the Coulomb-related divergence. On the other hand, one might argue that an exact computation should not exhibit any divergence, for the following

reason: since the liberated electron starts its orbit near its parent ion, when it returns it will scatter at a moderate impact parameter, so it will never actually experience the infinite range of the Coulomb potential. Therefore, one is physically justified to cut off the Coulomb potential at a safe distance away from the atom, thereby eliminating any divergence and accomplishing a term-by-term convergence of any expansion [25].

In this Letter, in the time-dependent case, we will take a different route. As it will turn out, the fact that the atomic ground state has a finite lifetime due to ionization is sufficient to remove the divergent denominators that cause the problems. Namely, in the  $S$ -matrix theory, the depletion of the bound state can be introduced by inserting a decay factor into the phase of the transition matrix element (1b), by replacing [26]

$$I_p t' \rightarrow I_p t' + \frac{i}{2} \int_{-T/2}^{t'} d\tau w(\tau), \quad (4)$$

where we consider the interaction between the atom and the laser pulse adiabatically turned on at time  $-T/2$ . Here, in analogy with Ref. [26],  $w(\tau)$  is the time-dependent ionization rate of the ground state. Using the saddle-point approximation in the integral over  $t'$  in (1b), one now gets the following equation for the tunneling process

$$\frac{1}{2} [\mathbf{p}' - \mathbf{A}(t')]^2 = -I_p - \frac{i}{2} w(t'). \quad (5)$$

The real part of the additional term  $w(t')$  explicitly gives a finite width to the photoelectron momentum, as follows: we approximate  $w(t')$  by the time-independent depletion rate  $\Gamma$  of the ground state. Then, the energy denominator in Eq. (2) is replaced by  $p'^2 - \mathcal{E}_n - i\Gamma/2$ , which is sufficient to remove the divergence, since  $p$  and  $p'$  are real. Note that the solutions  $t'$  of the saddle-point equation (5) are complex (as they already are for  $\Gamma = 0$ ) [26], which is related to the electron being liberated by tunneling.

The bottom line of this procedure is that introducing into the theory an element of reality—the fact that the ground state decays due to the action of the laser field—is sufficient to remove all problems and to generate term-by-term convergence. Moreover, as shown in Ref. [26], the depletion of the ground state is introduced in a self-consistent manner. For given laser parameters, the ground-state decay rate  $\Gamma$  is a well-defined number, which must be determined, in principle, in a self-consistent fashion in parallel with the expansion (1), so there is no need to guess a screening constant for the calculation. Since it is impossible to calculate the whole  $S$ -matrix expansion, we need to obtain a value of  $\Gamma$  by different means. We employ the Coulomb-corrected SFA, which is known to be quantitatively consistent with a numerical solution of the TDSE [27]. Equally well, we could have used the TDSE or inserted a value deduced from experiment. We remark that the calculated spectrum is not very sensitive to the value of  $\Gamma$ , as long as

$\Gamma$  is small, which is the case for the intensity chosen in this Letter.

The experiments were conducted using argon and xenon under various laser conditions. A midinfrared beam with a  $1/e^2$  diameter of 15 mm is focused by a 100 mm focal-length  $\text{CaF}_2$  lens into a vacuum chamber housing a 54 cm time-of-flight electron or ion spectrometer. The 40-mm-diameter  $\mu$ -channel plate detector provides a collection angle of 4 deg. More details can be found in Refs. [21,28]. For argon, the LES is studied for fixed laser wavelength (2  $\mu\text{m}$ ) and three different intensities [see Fig. 1(b)]. For xenon in Fig. 1(d),  $U_p$  is held constant by varying both wavelength (1.7, 2, and 2.3  $\mu\text{m}$ ) and intensity. Figure 1(f) shows results for xenon for fixed wavelength (3.6  $\mu\text{m}$ ) and different intensities.

For these various conditions, the theoretical results given by the second-order amplitude  $T^{(2)}$  [29] reproduce the low-energy structure (left-hand panels of Fig. 1) observed in the experiments (right-hand panels of Fig. 1) while the structure is absent in the first-order calculations, i.e.,  $T^{(1)}$  (dashed lines; all first-order results are shifted so that they agree with the second-order calculation at energies above the LES). It is noteworthy that, for the best consistency between experiment and theory, laser intensities used for the theoretical evaluations are 30%–50% less than those used in the experiments. This discrepancy may be partly due to uncertainty in the experimental intensity calibration (20%) and focal volume distribution averaging (a Gaussian distribution is assumed in the calculation). Moreover, as discussed above, the higher-order terms neglected in the  $S$ -matrix expansion may also contribute.

Two interesting features are apparent in Fig. 1: (i) the experimental studies show—and this is reproduced by the

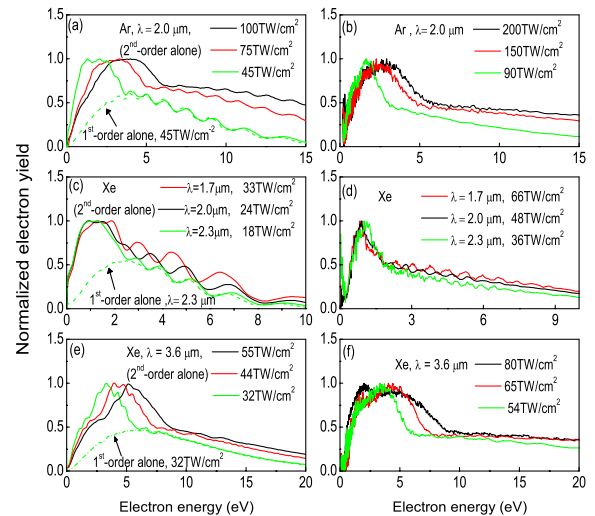


FIG. 1 (color online). Low-energy photoelectron energy spectra of Ar [(a),(b)] and Xe [(c)–(f)] in a midinfrared laser field. (a),(c),(e) Calculated from Eqs. (1b) (solid line) and (1a) (dashed line); (b),(d),(f) experimental results.

calculations—that the high-energy boundary  $E_H$  of the LES is well defined and has a strong dependence on the intensity, and (ii) the profile of the LES remains the same for fixed  $U_p$ , irrespective of the laser wavelength [see Figs. 1(c) and 1(d)]. In Ref. [21] it was observed that  $E_H \propto \gamma^{-1.8}$  regardless of the species, which is consistent with available TDSE calculations. However, no clear interpretation was offered. The present calculation predicts the scaling  $E_H \propto \gamma^{-1.5}$  or, alternatively,  $E_H \propto U_p^{3/4}$  (Fig. 2). Neither the calculation nor the available data allows us to discriminate between these two scalings. It is noteworthy that the systematic discrepancy between theoretical and experimental results due to, e.g., the calibration of intensity, does not affect the scaling law. According to our model, the LES originates from the photoelectron–parent-ion interaction. If the effect of the Coulomb potential were independent of the electron kinetic energy,  $E_H$  would scale as  $\gamma^{-2}$  or  $U_p$ . However, since the effect decreases with increasing kinetic energy, the scaling reduces to about  $\gamma^{-1.5}$  or  $U_p^{3/4}$ . The second-order  $S$ -matrix calculation therefore sheds some new light on the scaling and allows us to appreciate the dependence of the Coulomb effect on the photoelectron energy.

A crucial question is under which conditions the LES becomes observable in the ATI spectrum. Our analysis of the scaling of the upper boundary  $E_H$  of the LES shows that it is located at an energy much below  $U_p$ . This implies that the LES is well developed only when  $U_p$  is sufficiently large. Moreover, to distinguish the LES from the ATI peaks in the spectrum requires  $U_p \gg \omega$  (the laser frequency). These conditions are usually fulfilled in the tunneling regime and, in this regime, the individual ATI peaks, which

obstruct the visibility of the LES, are always smeared out due to focal-volume averaging.

Although the theory proposed in this Letter consistently explains the LES profiles observed in recent tunneling ionization experiments [21,22], several questions remain to be resolved. One concerns the significance of the higher-order terms in the expansion (1). Surely, in the present time-dependent case they will not merely contribute a phase as they do for time-independent Coulomb scattering [Eq. (3)]. In addition, although the two experiments [21,22] agree on the structure of the LES, Ref. [22] reports a sharp peak below 1 eV—definitely below the LES—in all of the measurements regardless of laser wavelength and intensity, which was absent in Ref. [21] as well as in the theoretical calculation in this Letter. This peak, which may be referred to as the very-low-energy structure (VLES) [30], was also reproduced in semiclassical and TDSE analysis, in which it was attributed to the relatively strong influence of the Coulomb potential on the outgoing photoelectrons with low kinetic energy [22,30,31]. This semiclassical effect may in our model be related to multiple scattering of the photoelectron in the Coulomb field of the parent ion. Our current second-order analysis did not generate this peak, suggesting it may be a consequence of the high-order terms here neglected. This will be pursued in future work.

How does the present simulation of the LES compare with earlier explanations? Owing to the peculiar nature of the Coulomb potential, this question is not easy to answer. Apparently, our theory—if interpreted in terms of the saddle-point approximation and the standard quantum orbits—does not incorporate the effect of the binding potential on the trajectories of the liberated electrons, which appears as the origin of the LES in Refs. [31–34]. This would imply that first-order Coulomb scattering of *plane-wave electrons* is sufficient to generate the LES. However, (1) we did not use the saddle-point approximation and, moreover, (2) the latter yields for low energy additional very short orbits (the so-called  $L$  orbits [35]) whose significance has not been explored in any detail. It is possible that in a quantum mechanical  $S$ -matrix description of ATI the interplay of the laser field and the Coulomb field is already satisfactorily captured in the first Born approximation.

In summary, a calculation of the lowest-order rescattering term (analogous to the lowest-order Born approximation) in a quantum mechanical  $S$ -matrix expansion of the ionization amplitude was presented and compared with extensive experimental data for various atoms, wavelengths, and intensities, which display the recently discovered low-energy structure. The calculation was carried out for very low momenta of the liberated electron and for an unscreened Coulomb potential. It reproduces many features of the data, including their wavelength and intensity dependence and the corresponding scaling. Technically, divergences due to the long-range Coulomb potential,

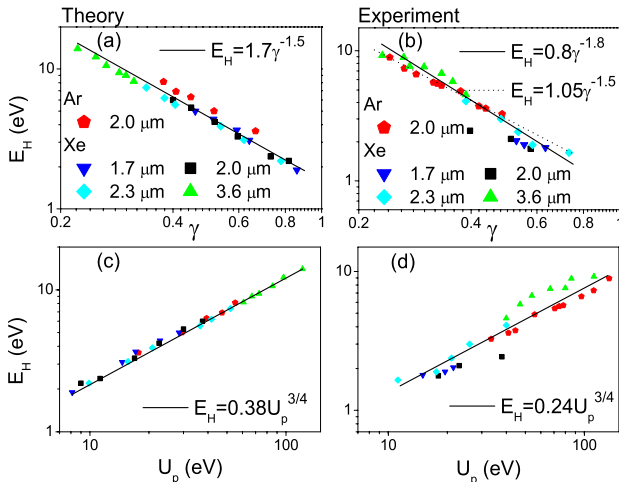


FIG. 2 (color online). The dependence of the LES high-energy boundary  $E_H$  on the Keldysh parameter  $\gamma$  and the ponderomotive energy  $U_p$  for various atoms and wavelengths. Left-hand column: Theoretical results; right-hand column: experimental results.

which are normally encountered in high-order terms of the  $S$ -matrix expansion, were removed by taking into account the actual value of the depletion of the atomic ground state due to ionization. It is proposed that to some extent the lowest-order rescattering term provides an “effective” description of forward rescattering and that the inclusion of higher-order terms may neither be necessary nor even desirable, in the same way that the first-order Born approximation yields the exact Coulomb scattering cross section.

This work was partially supported by the National Basic Research Program of China (No. 2013CB922201 and No. 2011CB8081002) and NNSFC (No. 11074026, No. 11175227, and No. 11105205) and Shanghai Supercomputer Center of China. The work at The Ohio State University was performed with support from the National Science Foundation under Contract No. PHY-1004778 and the Army Research Office.

\*fanjy@umd.edu

†chen\_jing@iapcm.ac.cn

- [1] P. Agostini, F. Fabre, G. Mainfray, G. Petite, and N. K. Rahman, *Phys. Rev. Lett.* **42**, 1127 (1979).
- [2] For a review, see, e.g., W. Becker, F. Grasbon, R. Kopold, D. B. Milošević, G. G. Paulus, and H. Walther, *Adv. At. Mol. Opt. Phys.* **48**, 35 (2002).
- [3] L. V. Keldysh, *Zh. Eksp. Teor. Fiz.* **47**, 1945 (1964) [*Sov. Phys. JETP* **20**, 1307 (1965)].
- [4] P. Kruit, J. Kimman, H. G. Muller, and M. J. van der Wiel, *Phys. Rev. A* **28**, 248 (1983).
- [5] H. R. Reiss, *Phys. Rev. A* **22**, 1786 (1980).
- [6] H. B. van Linden, van den Heuvel, and H. G. Muller, in *Multiphoton Processes*, edited by S. J. Smith, and P. L. Knight (Cambridge University Press, Cambridge, England, 1987), pp. 25–34.
- [7] P. B. Corkum, N. H. Burnett, and F. Brunel, *Phys. Rev. Lett.* **62**, 1259 (1989).
- [8] G. G. Paulus, W. Nicklich, H. Xu, P. Lambropoulos, and H. Walther, *Phys. Rev. Lett.* **72**, 2851 (1994).
- [9] K. J. Schafer, B. Yang, L. F. DiMauro, and K. C. Kulander, *Phys. Rev. Lett.* **70**, 1599 (1993).
- [10] P. B. Corkum, *Phys. Rev. Lett.* **71**, 1994 (1993).
- [11] F. M. H. Faisal, *J. Phys. B* **6**, L89 (1973).
- [12] J. Chen and C. H. Nam, *Phys. Rev. A* **66**, 053415 (2002).
- [13] R. Moshhammer, J. Ullrich, B. Feuerstein, D. Fischer, A. Dorn, C. D. Schröter, J. R. Crespo Lopez-Urrutia, C. Hoehr, H. Rottke, C. Trump, M. Wittmann, G. Korn, and W. Sandner, *Phys. Rev. Lett.* **91**, 113002 (2003).
- [14] K. I. Dimitriou, D. G. Arbo, S. Yoshida, E. Persson, and J. Burgdörfer, *Phys. Rev. A* **70**, 061401(R) (2004).
- [15] Z. Chen, T. Morishita, A.-T. Le, M. Wickenhauser, X.-M. Tong, and C. D. Lin, *Phys. Rev. A* **74**, 053405 (2006).
- [16] L. Guo, J. Chen, J. Liu, and Y. Q. Gu, *Phys. Rev. A* **77**, 033413 (2008).
- [17] A. Rudenko, K. Zrost, C. D. Schröter, V. L. B. de Jesus, B. Feuerstein, R. Moshhammer, and J. Ullrich, *J. Phys. B* **37**, L407 (2004).
- [18] A. S. Alnaser, C. M. Maharjan, P. Wang, and I. V. Litvinyuk, *J. Phys. B* **39**, L323 (2006).
- [19] F. H. M. Faisal and G. Schlegel, *J. Phys. B* **38**, L223 (2005).
- [20] F. H. M. Faisal and G. Schlegel, *J. Mod. Opt.* **53**, 207 (2006).
- [21] C. I. Blaga, F. Catoire, P. Colosimo, G. G. Paulus, H. G. Muller, P. Agostini, and L. F. DiMauro, *Nat. Phys.* **5**, 335 (2009).
- [22] W. Quan, Z. Lin, M. Wu, H. Kang, H. Liu, X. Liu, J. Chen, J. Liu, X. T. He, S. G. Chen, H. Xiong, L. Guo, H. Xu, Y. Fu, Y. Cheng, and Z. Z. Xu, *Phys. Rev. Lett.* **103**, 093001 (2009).
- [23] For example, see A. Gazibegović-Busuladžić, D. B. Milošević, W. Becker, B. Bergues, H. Hultgren, and I. Y. Kiyani, *Phys. Rev. Lett.* **104**, 103004 (2010), and references therein.
- [24] A. Messiah, *Quantum Mechanics* (North-Holland, Amsterdam, 1964), Vol. 1.
- [25] D. B. Milošević and F. Ehlötzky, *Phys. Rev. A* **57**, 5002 (1998).
- [26] M. Lewenstein, Ph. Balcou, M. Y. Ivanov, A. L’Huillier, and P. B. Corkum, *Phys. Rev. A* **49**, 2117 (1994).
- [27] A. Becker, L. Plaja, P. Moreno, M. Nurhuda, and F. H. M. Faisal, *Phys. Rev. A* **64**, 023408 (2001).
- [28] P. Colosimo, G. Doumy, C. L. Blaga, J. Wheeler, C. Hauri, F. Catoire, J. Tate, R. Chirila, A. M. March, G. G. Paulus, H. G. Muller, P. Agostini, and L. F. DiMauro, *Nat. Phys.* **4**, 386 (2008).
- [29] Our presentation so far, especially Eqs. (2), (4), and (5), was independent of the gauge. For the numerical evaluation, we apply velocity gauge using the pole approximation similar to Ref. [16], for simplicity.
- [30] C. Y. Wu, Y. D. Yang, Y. Q. Liu, Q. H. Gong, M. Wu, X. Liu, X. L. Hao, W. D. Li, X. T. He, and J. Chen, *Phys. Rev. Lett.* **109**, 043001 (2012).
- [31] A. Kästner, U. Saalmann, and J. M. Rost, *Phys. Rev. Lett.* **108**, 033201 (2012).
- [32] C. Liu and K. Z. Hatsagortsyan, *Phys. Rev. Lett.* **105**, 113003 (2010).
- [33] T. M. Yan, S. V. Popruzhenko, M. J. J. Vrakking, and D. Bauer, *Phys. Rev. Lett.* **105**, 253002 (2010).
- [34] C. Lemell, K. I. Dimitriou, X.-M. Tong, S. Nagele, D. V. Kartashov, J. Burgdörfer, and S. Gräfe, *Phys. Rev. A* **85**, 011403(R) (2012).
- [35] D. B. Milošević and W. Becker, *Phys. Rev. A* **66**, 063417 (2002).